

Neuron, Volume 79
Supplemental Information

**Potassium Channels Control the Interaction
between Active Dendritic Integration Compartments
in Layer 5 Cortical Pyramidal Neurons**

Mark T. Harnett, Ning-Long Xu, Jeffrey C. Magee, and Stephen R. Williams

Inventory of Supplemental Information

Contains: 1 Supplemental Table and 9 Supplemental Figures

— Statistical Methods and Results.

— Table S1, linked to Figure 4: Potassium channel blockers do not alter dendritic resting membrane potential and apparent input resistance.

— Figure S1, linked to Figures 1 & 2: Site of generation of apical dendritic trunk and tuft spikes. This figure shows analysis of the time-difference between regenerative dendritic spikes when simultaneously recorded at apical dendritic trunk, apical dendritic nexus, and apical dendritic tuft sites.

— Figure S2, linked to Figure 2: Current-evoked apical dendritic tuft spikes are compartmentalized and mediated by sodium channels. This figure illustrates the voltage compartmentalization and weak impact of apical dendritic tuft spikes evoked by simulated EPSPs, together with analysis of the ion channels underlying current-evoked apical dendritic tuft spikes.

— Figure S3, linked to Figure 2: Generation and compartmentalization of apical dendritic tuft spikes evoked by rapid, multi-site two-photon glutamate uncaging. This figure shows that glutamate uncaging evoked regenerative activity at apical dendritic sites is mediated by the activation of NMDA receptors, and that these supra-linear synaptic responses are highly compartmentalized in the apical dendritic tuft.

— Figure S4, linked to Figure 3: Properties of apical dendritic potassium channels. This figure illustrates the voltage- and time-dependent properties of potassium channels recorded in outside-out and cell-attached patches from the apical dendritic nexus and tuft of L5B pyramidal neurons.

— Figure S5, linked to Figure 4: Potassium channel blockers do not perturb somatically recorded action potentials. This figure summarises the effects of K_v

channel blockers on somatically recorded APs and dendritically recorded back-propagating APs.

— **Figure S6, linked to Figure 4: Blockade of potassium channels by barium selectively controls apical dendritic excitability.** This figure summarises the results from simultaneous somatic and apical dendritic recordings showing that barium (50 μ M) leads to a transformation of apical dendritic, but not somatic excitability.

— **Figure S7, linked to Figure 5: Blockade of potassium channels does not increase dendritic trunk calcium signalling generated by isolated dendritic trunk spikes.** This figure illustrates the local calcium signalling generated by apical dendritic trunk spikes under control and when K_V channels were blocked by a range of agents. The driving current was carefully adjusted to match the nexus recorded voltage waveforms and calcium signalling under the indicated conditions.

— **Figure S8, linked to Figure 8: Barium controls dendritic tuft calcium signalling evoked during behaviour consistently in all animals.** This figure shows the reversible enhancement of the occurrence, amplitude and area of dendritic tuft calcium signals by the local application of barium to the surface of the neocortex in each animal used in the study.

— **Figure S9, linked to Figure 8: In vivo barium application enhances the area of calcium signals throughout the dendritic tuft.** This summary figure shows the reversible enhancement of the total area of calcium signals per behavioural trial for all imaging regions of interest.

Statistical methods:

Statistical analysis included: Student's *t* test and ANOVA with Bonferroni's multiple comparison test. Normality of distribution was tested using the Kolmogorov-Smirnov test with Dallal-Wilkson-Lillie post test. Statistical significance was accepted at the level of $\alpha < 0.01$. All values are reported as mean \pm SEM. The statistical results are summarised below.

Statistical results:

Figure	Test	Conditions	T and P value
3 panel J	Paired Student's <i>t</i> test (two tailed).	Con vs Quin – peak Con vs Quin – ss Con vs 4-AP – peak Con vs 4-AP – ss Quin vs 4-AP – peak Quin vs 4-AP – ss Con vs Barium – peak Con vs Barium – ss	T = 5.302, P<0.0001 T = 5.214, P<0.0001 T = 8.214, P<0.0001 T = 0.438, P>0.05 T = 10.50, P<0.0001 T = 0.185, P>0.05 T = 8.738, P<0.001 T = 4.369, P<0.01
4 panel H	ANOVA with Bonferroni's multiple Comparisons.	Con vs TTX TTX vs Quin Quin vs Nickel	T = 0.805, P>0.05 T = 17.04, P<0.001 T = 6.573, P<0.001
6 panel D	Paired Student's <i>t</i> test (two tailed).	Con vs Quin Tuft area Trunk area	T = 10.56, P<0.0001 T = 7.554, P<0.0001
6 panel E	Paired Student's <i>t</i> test (two tailed).	Con vs Quin Tuft rheobase Trunk rheobase	T = 6.482, P<0.0001 T = 6.000, P<0.0001
6 panel G		Con vs Quin Con vs Barium	
7 panel B	ANOVA with Bonferroni's multiple Comparisons.	Difference in firing rate Con vs Quin. Average current: 0.0526318 0.116883 0.18114 0.245002 0.30944 0.373627 0.437922 0.502094 0.566716 0.631166 0.695727 0.759659 0.824252 0.888738 0.952828 1.01696	T = 0.5043, P > 0.05 T = 0.937, P > 0.05 T = 1.945, P > 0.05 T = 1.513, P > 0.05 T = 2.233, P > 0.05 T = 2.666, P > 0.05 T = 3.530, P < 0.01 T = 3.891, P < 0.01 T = 4.323, P < 0.001 T = 4.323, P < 0.001 T = 4.539, P < 0.001 T = 4.153, P < 0.001 T = 3.849, P < 0.01 T = 4.025, P < 0.01 T = 3.379, P < 0.05 T = 3.481, P < 0.05

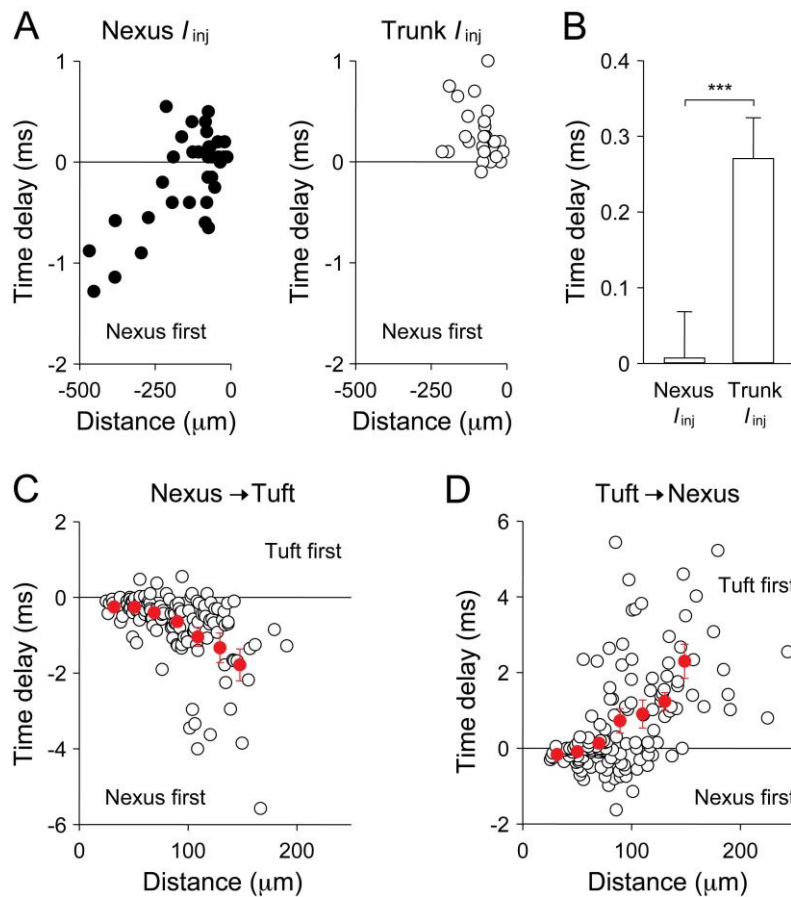
		1.08122 1.14484 1.20932 1.2737	T = 2.933, P > 0.05 T = 3.069, P < 0.05 T = 1.064, P > 0.05 T = 0.479, P > 0.05
7 panel C	ANOVA with Bonferroni's multiple Comparisons.	Difference in dendritic area, Con vs Quin. Average current: 0.0526318 0.116883 0.18114 0.245002 0.30944 0.373627 0.437922 0.502094 0.566716 0.631166 0.695727 0.759659 0.824252 0.888738 0.952828 1.01696 1.08122 1.14484 1.20932 1.2737	T = 0.412, P > 0.05 T = 0.702, P > 0.05 T = 0.888, P > 0.05 T = 1.005, P > 0.05 T = 1.337, P > 0.05 T = 1.589, P > 0.05 T = 2.149, P > 0.05 T = 2.581, P > 0.05 T = 3.296, P < 0.05 T = 3.624, P < 0.01 T = 4.829, P < 0.001 T = 5.899, P < 0.001 T = 6.692, P < 0.001 T = 7.261, P < 0.001 T = 5.967, P < 0.001 T = 6.441, P < 0.001 T = 6.453, P < 0.001 T = 5.656, P < 0.001 T = 5.360, P < 0.001 T = 5.018, P < 0.001
8 panel F	ANOVA with Bonferroni's multiple Comparisons	Con vs Barium Barium vs wash Con vs wash	T = 8.089, P<0.001 T = 4.511, P<0.001 T = 3.578, P<0.01
8 panel G	ANOVA with Bonferroni's multiple Comparisons	Data pooled for all ROI: Con vs Barium Barium vs wash Con vs wash	T = 5.762, P<0.001 T = 4.474, P<0.001 T = 1.287, P>0.05

Supplemental Table 1: Potassium channel blockers do not alter dendritic resting membrane potential and apparent input resistance.

Apical dendritic nexus	Control	Quinidine (25 μ M)	Control	Barium (20-50 μ M)
Resting membrane potential	-57.0 ± 0.3 mV $n = 61$	-57.2 ± 0.4 mV $n = 61$	-56.0 ± 0.4 mV $n = 25$	-55.7 ± 0.5 mV $n = 25$
Peak input resistance [#]	20.4 ± 1.3 M Ω $n = 15$	21.6 ± 1.2 M Ω $n = 15$	20.2 ± 1.3 M Ω $n = 11$	20.5 ± 1.3 M Ω $n = 11$
Steady-state input resistance [#]	9.8 ± 0.9 M Ω $n = 15$	10.5 ± 0.8 M Ω $n = 15$	11.1 ± 0.6 M Ω $n = 11$	11.7 ± 0.6 M Ω $n = 11$
I_H -mediated voltage sag [#]	10.6 ± 0.6 mV $n = 15$	11.1 ± 0.6 mV $n = 15$	9.1 ± 0.8 mV $n = 11$	8.8 ± 0.9 mV $n = 11$

[#]Dual nexus whole-cell recordings used to independently inject current and record voltage, pipette separation < 10 μ m. Input resistance calculated in response to a 1 s, -1 nA current step.

Values represent mean \pm SEM. Paired groups are not significantly different (Student's T-



test).

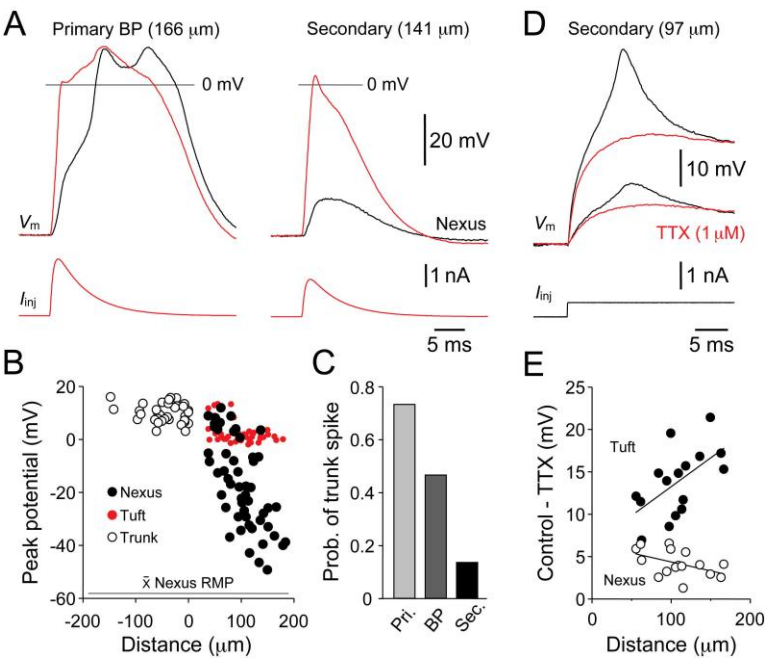
Supplemental Figure 1: Site of generation of apical dendritic trunk and tuft spikes

(A) Time delay (measured at peak amplitude) of apical dendritic trunk spikes evoked and recorded at the apical dendritic nexus by rheobase positive current steps and independently recorded from proximal apical dendritic trunk sites (left graph) and spikes evoked at proximal apical dendritic trunk sites and independently recorded from the nexus. Distance refers to electrode separation, and zero corresponds to the location of the nexus electrode.

(B) Summary of the time delay for apical dendritic trunk spikes evoked by nexus or distal apical dendritic trunk positive currents steps (average electrode separation = $88 \pm 10 \mu\text{m}$, $n = 26$, $*** = P < 0.001$, Student's t test). Note that when evoked from the nexus, trunk spikes occur on average almost simultaneously at both recording sites. In the same recordings trunk spikes evoked by distal apical dendritic trunk current steps are on average first recorded at this site, indicating that apical dendritic trunk spikes are initiated in the region of the most distal $200 \mu\text{m}$ of the apical dendritic trunk. Values represent mean \pm SEM

(C) Time-delay between apical dendritic trunk spikes evoked at the nexus and independently recorded from the apical dendritic tuft. The red symbols indicate data pooled into $20 \mu\text{m}$ bins.

(D) Time delay between regenerative spikes evoked and recorded at apical dendritic tuft sites by rheobase positive currents steps and independently recorded from the nexus of the apical dendritic trunk. The red symbols indicate data pooled into $20 \mu\text{m}$ bins. Note that regenerative activity occurs first at apical dendritic tuft sites when recordings are made $> 70 \mu\text{m}$ from the nexus.



Supplemental Figure 2: Current-evoked apical dendritic tuft spikes are compartmentalized and mediated by sodium channels

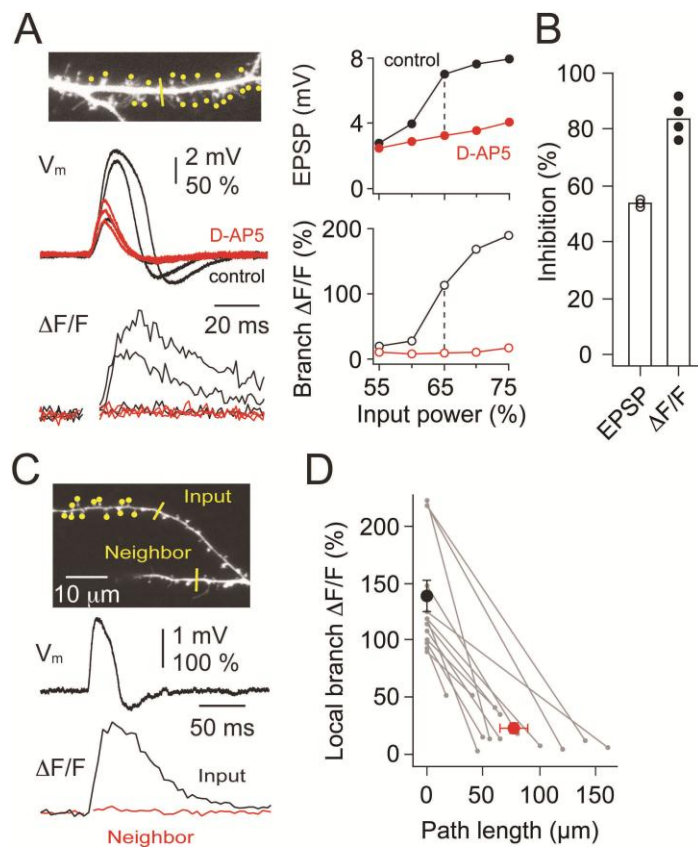
(A) Simultaneous recording from the nexus (black traces) and apical dendritic tuft of a complex spike initiated at a primary apical dendritic tuft branch point (left traces) and an isolated tuft spike initiated from a secondary apical dendritic tuft site by the injection of EPSC shaped current waveforms (lower traces). Note that the initial voltage response evoked by a simulated EPSC delivered to the primary apical dendritic tuft branch point (red trace) crosses 0 mV, and is followed by the recruitment of an apical dendritic trunk spike (black trace).

(B) Pooled data describing the impact of tuft generated responses at the nexus (black symbols). The amplitude of voltage responses at the nexus was measured at peak amplitude. The red symbols show the peak amplitude of tuft voltage responses measured in a 3 ms time-window following the peak of the driving excitatory postsynaptic current. Note, that the local amplitude of events recorded at the tuft site of generation are close to 0 mV. The open symbols show the peak amplitude of dendritic trunk spikes evoked from apical dendritic trunk sites proximal to the nexus (negative distances). Distance refers to separation between recording electrodes.

(C) The probability that voltage responses which reached 0 mV at the apical dendritic tuft site of generation evoke a dendritic trunk spike, when simulated excitatory postsynaptic potentials were generated at primary, primary branch point and secondary apical dendritic tuft sites.

(D) Simultaneous apical dendritic tuft and nexus recording under control and in the presence of the sodium channel blocker Tetrodotoxin (TTX, 1 μ M).

(E) Distance-dependent increase in the amplitude of TTX-sensitive spikes in the apical dendritic tuft, but decrease in their impact at the nexus.



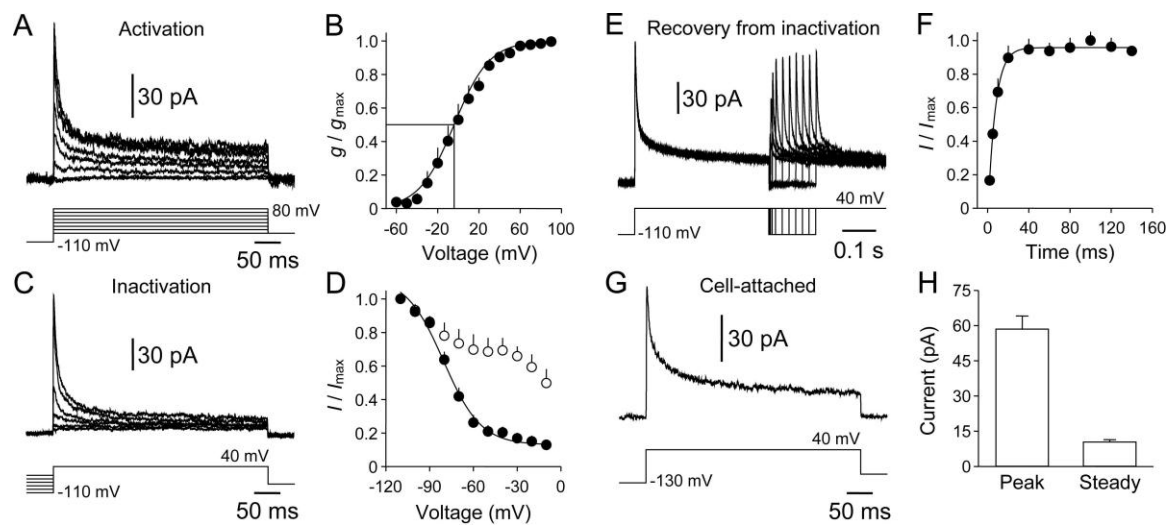
Supplemental Figure 3: Generation and compartmentalization of apical dendritic tuft spikes evoked by rapid, multi-site two-photon glutamate uncaging

(A) Supra-threshold Oregon Green Bapta-6F signals are blocked by the NMDA receptor antagonist D-AP5 (50 μ M). The nexus recorded voltage (V_m) and branch Oregon Green Bapta-6F signals were generated in response to multi-site glutamate uncaging across a range of laser power to the heads of dendritic spines on a tertiary apical dendritic tuft branch (inset photomicrograph), under control conditions (black traces) and in the presence of D-AP5 (50 μ M, red traces). The inset graphs show the effects of D-APV on the amplitude of voltage responses (upper) and branch Oregon Green Bapta-6F signals (signals) across a range of uncaging laser power.

(B) Summary of the inhibition of voltage responses (EPSPs) and branch Oregon Green Bapta-6F signals by D-AP5.

(C) Compartmentalization of apical dendritic tuft branch calcium signals. A supra-threshold local Oregon Green Bapta-6F signal was recorded from a 4° apical dendritic branch that received multi-site glutamate uncaging (input), but the signal failed to propagate to a nearby sister branch (neighbour). The inset photomicrograph shows the sites of multi-site glutamate uncaging (spots) and line-scans. The nexus voltage recording (V_m) shows the characteristic waveform of a terminal tuft dendrite NMDA-mediated regenerative response.

(D) Summary of the attenuation of Oregon Green Bapta-6F signals from input sites to neighbouring apical dendritic tuft branches (n = 14 branches from 4 neurons, mean \pm SEM).



Supplemental Figure 4: Properties of apical dendritic potassium channels

(A) A family of ensemble channel currents generated in response to an incremental series of voltage steps recorded from a patch excised from a primary apical dendritic tuft site.

(B) Activation curve of ensemble potassium channel activity recorded from apical dendritic tuft sites. The amplitude of ensemble potassium channel activity was measured at peak amplitude and converted to conductance assuming a reversal potential of -86 mV (see Bekkers 2000a). The solid line represents a fit to the data with a single Boltzmann function with a voltage of half-maximal activation of -4 mV and slope factor of -17 mV.

(C) Steady-state inactivation of ensemble channel currents recorded from a patch excised from the nexus, generated in response to a test step to +40 mV which was preceded by a series of voltage steps (500 ms duration).

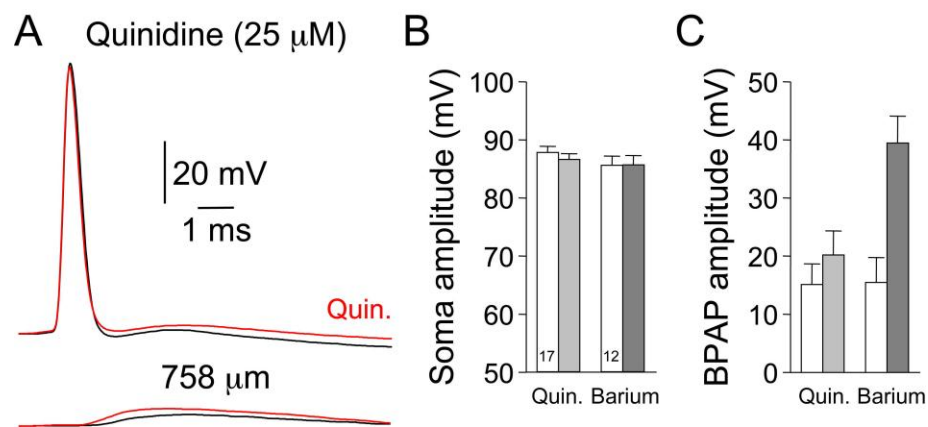
(D) Voltage dependence of inactivation measured at the peak (filled symbols) and steady-state (open symbols) of ensemble potassium channel activity. The line represents a fit by a Boltzmann function with added constant.

(E) Recovery from inactivation of the transient component of ensemble potassium channel activity recorded from a patch excised from the nexus.

(F) Pooled data describing the time-course of recovery from inactivation of the transient component, following the subtraction of the steady state component. The line represents a fit to the data by a single exponential function.

(G) Ensemble potassium channel activity recorded from the nexus in a cell-attached patch.

(H) Summary of the amplitude of ensemble potassium channel activity measured at the peak and steady-state in cell-attached patches recorded from the nexus and apical dendritic tuft sites ($n = 17$). For cell-attached recordings pipettes (open tip resistance of 10 to 12 M Ω) were filled with (in mM): 135 NaCl; 3 KCl; 10 HEPES; 2 MgCl₂; 1 CaCl₂; 0.5 CdCl₂; and 25 Glucose (pH 7.3-7.4; NaOH). Cell-attached patches were held at an intra-pipette holding potential of -20mV. All values represent mean \pm SEM.

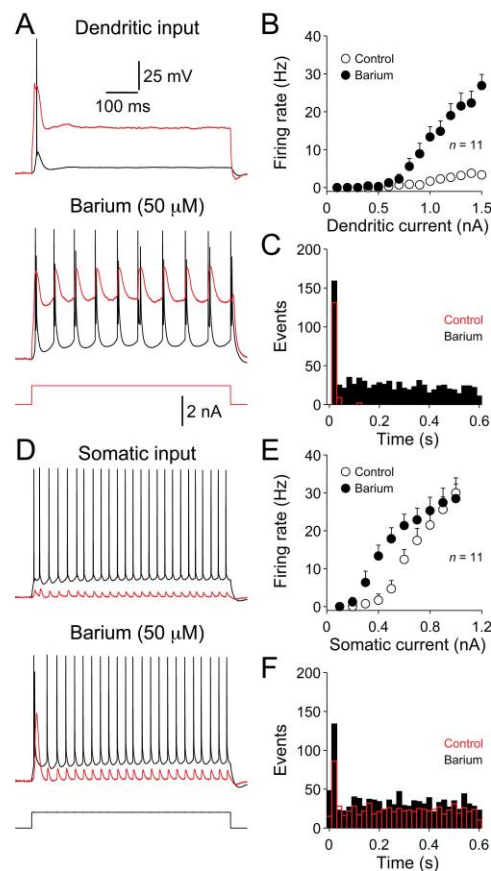


Supplemental Figure 5: Potassium channel blockers do not perturb somatically recorded action potentials

(A) Simultaneous somatic and apical dendritic nexus recording of action potential waveforms under control (black traces) and in the presence of Quinidine (25 μ M, red traces). Action potentials were generated in response to a step of positive current delivered at the soma.

(B) Summary data describing the effect of potassium channel blockers on the peak amplitude of action potentials recorded from the soma (Quinidine (25 μ M), barium (50 μ M)).

(C) The action of potassium channel blockers on the peak amplitude of action potentials recorded from the nexus of the apical dendritic trunk. Note that barium significantly enhanced the amplitude of back-propagating action potentials (barium: $P < 0.0005$, Student's t test). Values represent mean \pm SEM.



Supplemental Figure 6: Blockade of potassium channels by barium selectively controls apical dendritic excitability

(A) Simultaneous somatic (black) and apical dendritic nexus (red) recording of neuronal output evoked by a step of current delivered at the nexus under control and in the presence of the potassium channel blocker barium ($50 \mu\text{M}$).

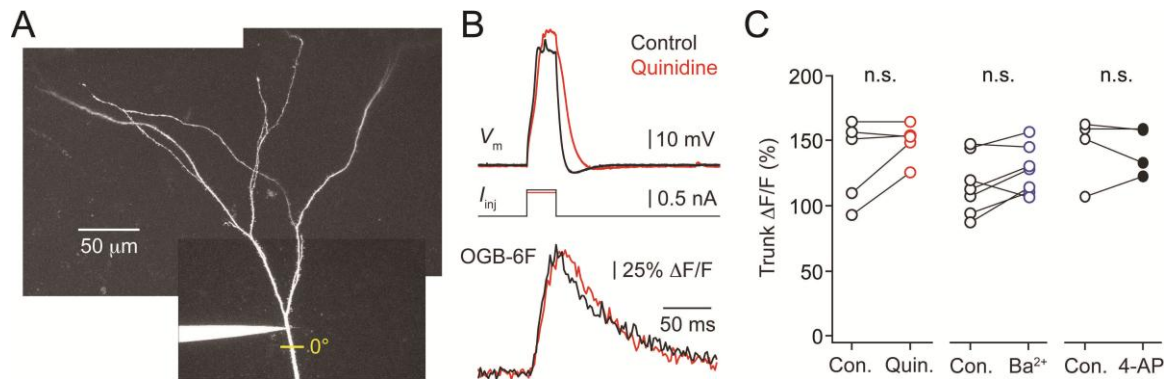
(B) Pooled nexus current-evoked axonal action potential output relationship under control (open symbols) and in barium (filled symbols). Firing rate was calculated as the number of action potentials per second.

(C) Pooled peri-stimulus time histogram of action potential firing evoked by apical dendritic current under control (red) and in barium (black).

(D) Action potential firing evoked by somatic current injection under control and in barium, same neuron as shown in A.

(E) Pooled somatic current-action potential output relationship.

(F) Pooled somatic current-evoked peri-stimulus time histogram of action potential firing. Values represent mean \pm SEM.

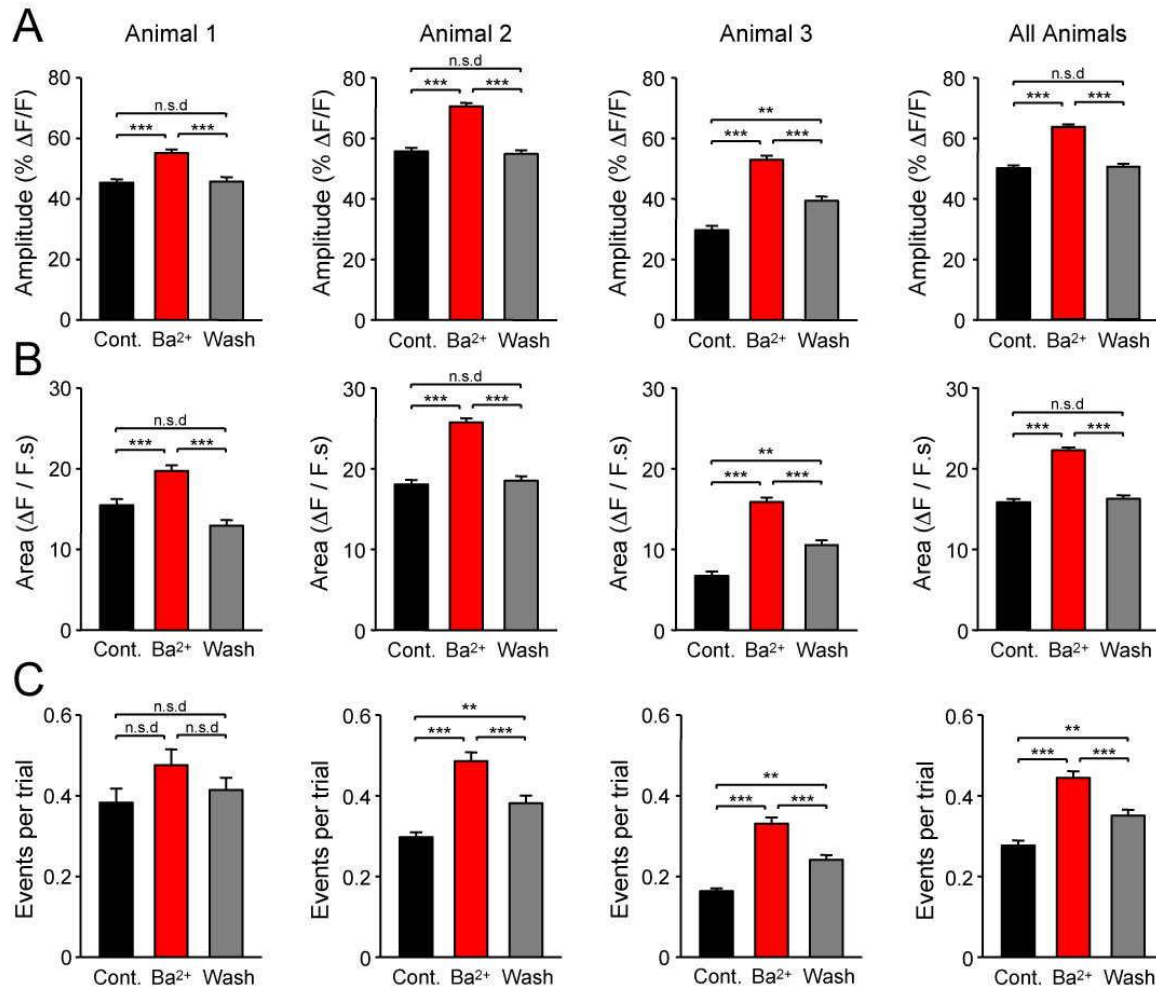


Supplemental Figure 7: Blockade of potassium channels does not increase dendritic trunk calcium signalling generated by isolated dendritic spikes

(A) Photomicrograph of the apical dendritic tuft of a layer 5B pyramidal neuron showing the placement of the recording electrode and position of the line-scan at the apical dendritic trunk (0°).

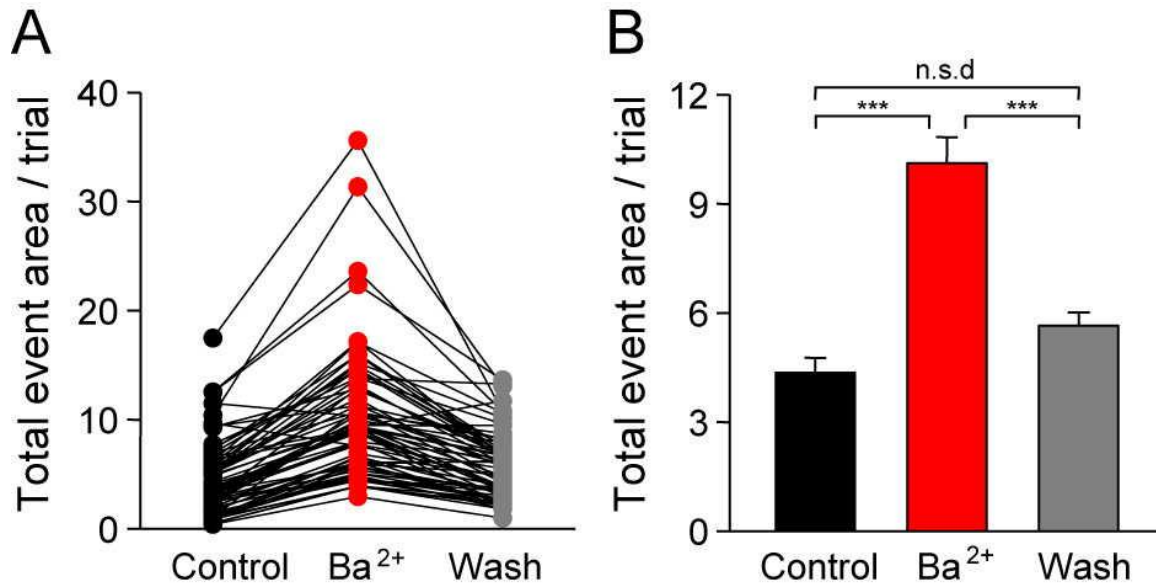
(B) Apical dendritic trunk spike (V_m) evoked by a threshold step of positive current (I_{inj}) under control (black traces) and in the presence of Quinidine (25 μ M, red traces). The lower traces show Oregon Green Bapta-6F calcium signals recorded from the apical dendritic trunk (position shown in A).

(C) Summary data showing the lack of a statistically significant (n.s., Student's t test) change in the peak amplitude of Oregon Green Bapta-6F signals recorded from the apical dendritic trunk under control (con) and in the presence of the potassium channel blockers Quinidine (25 μ M, red), barium (50 μ M, blue) and 4-aminopyridine (3 mM, black).



Supplemental Figure 8: Barium controls dendritic tuft calcium signalling evoked during behaviour consistently in all animals.

(A-C) The influence of barium (400 μ M) on the amplitude (panel A), area (panel B) and occurrence (panel C) of dendritic calcium signals recorded from regions of interest in each animal. The right hand graphs show data pooled across animals. Groups were analysed using one-way ANOVA and individual conditions tested with Bonferroni's multiple comparison test. ** = $P < 0.01$. *** = $P < 0.001$. n.s.d = not significantly different. All values represent mean \pm SEM.



Supplemental Figure 9: In vivo barium application enhances the area of calcium signals throughout the dendritic tuft.

(A) The influence of barium (400 μ M) on the total area of dendritic calcium signals per trial for 70 imaging regions of interest recorded from 3 animals. Note that barium enhanced the total area of calcium signals per trial in 68 of 70 regions of interest.

(B) Summary of the data presented in panel A. Groups were analysed using one-way ANOVA and individual conditions tested with Bonferroni's multiple comparison test. *** = $P < 0.001$. n.s.d = not significantly different. All values represent mean \pm SEM.